American Mineralogist, Volume 97, pages 1796–1803, 2012

Crystal structure of pseudojohannite, with a revised formula, $Cu_3(OH)_2[(UO_2)_4O_4(SO_4)_2](H_2O)_{12}$

Jakub Plášil,[1,2,*] Karla Fejfarová,[2] Kia Sheree Wallwork,[3] Michal Dušek,[2] Radek Škoda,[1] Jiří Sejkora,[4] Jiří Čejka,[4] František Veselovský,[5] Jan Hloušek,[6] Nicolas Meisser,[7] and Joël Brugger[8,9]

[1]Department of Geological Sciences, Faculty of Science, Masaryk University, Kotlářská 2, CZ-611 37, Brno, Czech Republic
[2]Institute of Physics ASCR, v.v.i., Na Slovance 2, CZ-182 21 Prague, Czech Republic
[3]Australian Synchrotron, 800 Blackburn Road, Clayton, Victoria 3168, Australia
[4]Department of Mineralogy and Petrology, National Museum, Cirkusová 1740, CZ-193 00, Prague 9, Czech Republic
[5]Czech Geological Survey, Geologická 6, CZ-152 00, Praha 5, Czech Republic
[6]U Roháčových kasáren 24, CZ-100 00, Praha 10, Czech Republic
[7]Musée de Géologie and Laboratoire des Rayons-X, Institut de Minéralogie et de Géochimie, UNIL, Anthropole, CH-1015 Lausanne-Dorigny, Switzerland
[8]South Australian Museum, North Terrace, Adelaide, South Australia 5000, Australia
[9]TRaX, School of Earth and Environmental Sciences, University of Adelaide, 5005 Adelaide, Australia

Abstract

The crystal structure of pseudojohannite from White Canyon, Utah, was solved by charge-flipping from single-crystal X-ray diffraction data and refined to an $R_{obs} = 0.0347$, based on 2664 observed reflections. Pseudojohannite from White Canyon is triclinic, $P\overline{1}$, with $a = 8.6744(4)$, $b = 8.8692(4)$, $c = 10.0090(5)$ Å, $\alpha = 72.105(4)°$, $\beta = 70.544(4)°$, $\gamma = 76.035(4)°$, and $V = 682.61(5)$ Å^3, with $Z = 1$ and chemical formula $Cu_3(OH)_2[(UO_2)_4O_4(SO_4)_2](H_2O)_{12}$. The crystal structure of pseudojohannite is built up from sheets of zippeite topology that do not contain any OH groups; these sheets are identical to those found in zippeites containing Mg^{2+}, Co^{2+}, and Zn^{2+}. The two Cu^{2+} sites in pseudojohannite are [5]- and [6]-coordinated by H_2O molecules and OH groups. The crystal structure of the pseudojohannite holotype specimen from Jáchymov was refined using Rietveld refinement of high-resolution powder diffraction data. Results indicate that the crystal structures of pseudojohannite from White Canyon and Jáchymov are identical.

Keywords: Pseudojohannite, zippeite group, uranyl sulfate, X-ray diffraction, crystal structure, chemical composition

Introduction

Pseudojohannite was described as a new mineral from Jáchymov (St. Joachimsthal), Western Bohemia, Czech Republic by Ondruš et al. (1997, 2003). In the original submission to the CNMNC IMA, its chemical formula was reported as $Cu_5(UO_2)_6(SO_4)_3(OH)_{16}(H_2O)_{14}$ and the refined triclinic unit-cell parameters were $a = 13.754(2)$, $b = 9.866(1)$, $c = 8.595(2)$ Å, $\alpha = 103.84(2)°$, $\beta = 90.12(2)°$, $\gamma = 106.75(2)°$, and $V = 1081.3(4)$ Å^3. Its name, pseudojohannite, expressed it is chemically and paragenetically related to the hydrated uranyl sulfate of copper, johannite, $Cu(UO_2)_2(SO_4)_2(OH)_2(H_2O)_8$ (Mereiter 1982). Later, based on a synchrotron powder diffraction study of the sample from Musonoï (Katanga, Democratic Republic of the Congo), Brugger et al. (2006) redefined the triclinic pseudojohannite unit-cell parameters as $a = 10.027(1)$, $b = 10.822(1)$, $c = 13.396(1)$ Å, $\alpha = 87.97(1)°$, $\beta = 109.20(1)°$, $\gamma = 90.89(1)°$, $V = 1371.9(5)$ Å^3, and $Z = 1$. From synchrotron powder data they were able to localize the uranium and sulfur atoms using direct-methods. They concluded that pseudojohannite is a member of the zippeite group, with characteristic U:S ratio 2:1 (Burns 2005; Brugger et al. 2003; Plášil et al. 2011a), and revised its chemical formula accordingly to $Cu_{6.5}[(UO_2)_4O_4(SO_4)_2]_2(OH)_5(H_2O)_{25}$.

Here we present the crystal structure of pseudojohannite from White Canyon, determined for the first time by single-crystal X-ray diffraction. We also provide an updated chemical composition of this mineral species. Furthermore, a Rietveld refinement of the crystal structure of pseudojohannite from the holotype specimen from Jáchymov, Czech Republic, was performed using high-quality synchrotron X-ray diffraction powder data. The results are compared with those obtained for pseudojohannite from White Canyon.

Occurrences

The crystal structure of pseudojohannite was determined from the specimen originating from Widowmaker mine, White Canyon, San Juan County, Utah, U.S.A. The sample is deposited in the collection of the Geological Museum of Lausanne (Switzerland) under the specimen number MGL 90939. The specimen was recovered from a rock of the size $4 \times 3 \times 2$ cm, consisting of silt containing lamellar coal with disseminated uraninite and chalcocite. On its surface and along cracks, the specimen is covered by secondary alteration minerals. Rich crystalline aggregates of pseudojohannite are composed of light greenish crystals elongated in one direction, measuring usually ~40 μm in length along this dimension (Fig. 1). Along with pseudojohannite,

* E-mail: plasil@fzu.cz

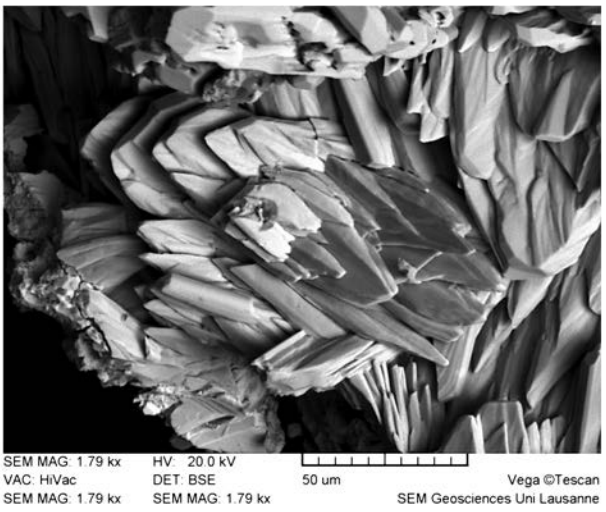

FIGURE 1. Crystals of pseudojohannite from White Canyon having typical crystal habit of zippeite group minerals. BSE image by N. Meisser (Vega Tescan).

johannite and natrozippeite have also been identified both by powder and single-crystal X-ray diffraction and EDS. Other samples with pseudojohannite also contain uranopilite and becquerelite.

A few pseudojohannite specimens were studied, including the holotype specimen, originating from the Jáchymov ore district, Czech Republic. The holotype specimen is deposited in the Mineralogical collection of the National Museum Prague (Czech Republic) under the specimen number P1P 1/2000. This specimen was found within a rich altered ore lens, consisting mainly of uraninite, pyrite, tennantite, and chalcopyrite (Ondruš et al. 1997, 2003). Over the time of ~30 years in the old mining adit, this uraninite ore lens underwent an alteration, and the exposed mineral surfaces and cracks were filled with the secondary uranyl sulfate copper minerals johannite and pseudojohannite along with other uranyl sulfates (e.g., magnesiozippeite and uranopilite) and other phases. Pseudojohannite forms rich, fine crystalline aggregates that are green in color and up to 5 mm thick; in some places pseudojohannite also forms coatings with an uneven surface, composed of crystals with sizes of ~10 μm (Fig. 2).

CHEMICAL COMPOSITION

The chemical composition of pseudojohannite samples was studied on carbon-coated polished sections using a Cameca SX100 electron microprobe operating in wavelength-dispersion mode, with an acceleration voltage of 15 kV, a current of 4 nA, and a beam diameter of 15 μm. The following X-ray lines and standards were selected to minimize line overlaps: *K*α lines: S (barite); Mg, Si (Mg_2SiO_4); *L*α lines: Cu (lammerite); *M*β lines: U (U metal). Peak counting times (CT) were 10–20 s for major elements, 40–60 s for minor to trace elements, and counting time on the background points was ½ CT. The measured intensities were converted to element concentrations using the "PAP" (Pouchou and Pichoir 1985) correction routine. High analytical totals were generally caused by water evaporation in high vacuum and heating of the analyzed spot by the electron beam. Element concentrations in weight percents, detection limits, and standard deviations on the averaged concentrations for the White Canyon and Jáchymov samples are given in Tables 1 and 2.

The chemical composition of pseudojohannite from White Canyon can be expressed by the empirical formula $(Cu_{3.07}Mg_{0.01})_{\Sigma 3.08}(UO_2)_{3.91}O_4[(SO_4)_{1.55}(SiO_4)_{0.47}]_{\Sigma 2.02}(OH)_{1.01}(H_2O)_{12}$, calculated as the average of 8 point analyses on the basis of 9 atoms in the empirical formula. Besides dominant Cu at cationic sites, only Mg was found at concentrations above detection limits. An elevated content of SiO_4^{4-} was measured, corresponding to up to ~0.6 apfu substitution for SO_4^{2-}. The higher contents of Si are responsible for the difference between 2 OH^- in the ideal formula of pseudojohannite and the 1 OH^- obtained here.

The results of the chemical analyses on the holotype specimen from Jáchymov are listed in Table 2. Although Cu^{2+} was the dominant cation, Mg^{2+} was also detected, in concentrations similar to those measured in the White Canyon samples. The chemical composition of pseudojohannite from Jáchymov can

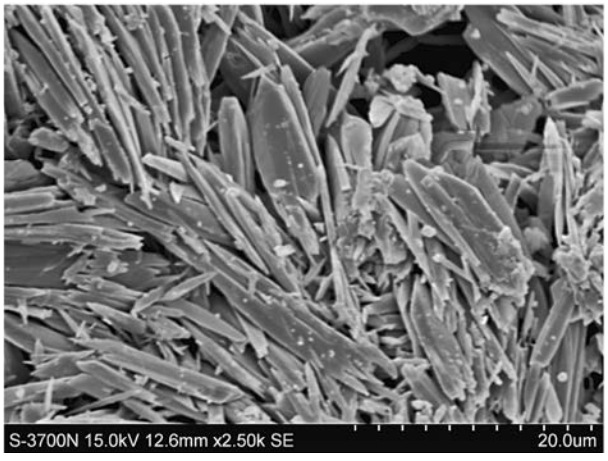

FIGURE 2. Minute pseudojohannite crystals on P1P 1/2000 holotype specimen, from Jáchymov deposited in collections of the National Museum in Prague. SE image by J. Sejkora (Hitachi S-3700N).

TABLE 1. Chemical composition of pseudojohannite (in wt%) from White Canyon

	Mean	Range	St.dev.
MgO	0.03	0.00–0.11	0.04
CuO	14.62	13.02–16.47	1.25
SiO_2	1.68	1.06–2.13	0.37
SO_3	7.43	6.38–8.39	0.59
UO_3	66.99	64.19–69.20	1.82
H_2O*	13.50	–	–
Total	104.24		
Mg	0.011		
Cu	3.066		
∑M-site	3.077		
SiO_4	0.465		
SO_4	1.549		
∑T-site	2.014		
UO_2^{2+}	3.908		
H_2O+OH	13.010		
M:T	1.527		
UO_2^{2+}:T	1.940		

Note: Mean = average composition on 1–8 point analyses, Range = range of 8 analyses, St.dev. = standard deviation of 8 analyses.
* H_2O = content in wt% calculated on the base of 12 H_2O present in the crystal structure + sum of OH^- inferred from charge balance. Coefficients of empirical formula calculated on the base of 9 atoms per formula.

TABLE 2. Chemical composition of pseudojohannite (in wt%) from Jáchymov (P1P 1/2000)

	Mean	Range	St.dev.
MgO	0.03	0.00–0.11	0.04
CuO	13.39	12.42–14.39	0.71
SiO_2	0.11	0.00–0.41	0.16
SO_3	8.41	8.02–8.72	0.23
UO_3	66.16	64.33–69.00	1.69
H_2O*	13.38	–	–
Total	101.48		
Mg	0.014		
Cu	2.986		
∑M-site	2.990		
SiO_4	0.033		
SO_4	1.863		
∑T-site	1.896		
UO_2^{2+}	4.104		
H_2O+OH	14.351		
M:T	1.575		
UO_2^{2+}:T	2.165		

Note: Mean = average composition on 1–5 point analyses, Range = range of 5 analyses, St.dev. = standard deviation of five analyses.
* H_2O = content in wt% calculated on the base of 12 H_2O present in the crystal structure + sum of OH^- inferred from charge balance. Coefficients of empirical formula calculated on the base of 9 atoms per formula.

be expressed by the empirical formula $(Cu_{2.99}Mg_{0.01})_{\Sigma 3.00}(UO_2)_{4.10}O_4[(SO_4)_{1.86}(SiO_4)_{0.03}]_{\Sigma 1.89}(OH)_{2.35}(H_2O)_{12}$, calculated as the average of 5 point analyses on the basis of 9 atoms in the empirical formula. Atoms of Si were also found to be entering tetrahedral sites, however in lower concentrations than in the White Canyon samples. The OH^- content obtained from charge balance is in accordance with the ideal pseudojohannite formula.

A combined TG/DTA measurement was performed using Stanton-Redcroft thermobalance TG-750 on the pseudojohannite holotype specimen (P1P 1/2000) from Jáchymov. Sample weight was 1.957 mg, heating rate 10 °C/min, with a dynamic air atmosphere 10 mL/min. The DTA analysis was performed using Blažek's apparatus, sample weight 8 mg, reference sample Al_2O_3, heating rate 10 °C/min and under a static air atmosphere. The results are presented by Brugger et al. (2006), and we provide a new interpretation of the analysis here. The dehydration and dehydroxylation processes during the heating of pseudojohannite are overlapping and proceed stepwise up to 625 °C, with a total weight loss of 13.85% (Table 3), corresponding to the release of 13 H_2O molecules (or 12 H_2O + 1 OH) from the structure. Endotherms at ~50 and ~105 °C are connected with stepwise dehydration of pseudojohannite. An endotherm at ~260 °C is related to dehydroxylation, while an exotherm at ~520–525 °C may be assigned to the destruction of the structure of probably yet X-ray amorphous and anhydrous pseudojohannite, and subsequent crystallization of β-UO_2SO_4. Such process was documented in similar case of thermal decomposition of johannite (Čejka 1999; Čejka et al. 1988; Sokol and Čejka 1992). Two further endotherms at 695 and 935 °C may be connected with stepwise decomposition of uranyl sulphate, with release of SO_3, and formation of copper uranates.

TABLE 3. Interpretation of thermal analysis of pseudojohannite (P1P 1/2000)

Temperature (°C)	Weight loss		Assignment
	(mg)	(%)	
20–200	0.173	8.84	~9 H_2O
200–625	0.098	5.01	~4 H_2O (3 H_2O + 2 OH) + ~0.5 O_2
625–800	0.090	4.60	~1 SO_3 + 0.1 O_2

CRYSTALLOGRAPHY

Single-crystal diffraction

A 0.10 × 0.07 × 0.02 mm prismatic light greenish crystal of pseudojohannite from White Canyon was selected for the single-crystal X-ray diffraction experiment. A set of intensity data was collected using an Oxford diffraction Gemini single-crystal diffractometer system equipped with an Atlas detector (monochromatic Mo$K\alpha$ radiation), and with fiber-optics Mo-Enhance collimator. The triclinic unit cell with a cell dimensions of a = 8.6744(4), b = 8.8692(4), c = 10.0090(5) Å, α = 72.105(4)°, β = 70.544(4)°, γ = 76.035(4)°, and V = 682.61(5) Å^3, with Z = 1, was chosen and refined using 5580 reflections within the CrysAlis Pro package (Agilent Technologies 2010). This smaller unit cell has approximately half of the unit-cell volume reported by Brugger et al. (2006). It is not unreasonable that powder diffraction was unable to identify this smaller cell due to the complexity of the triclinic diffraction pattern; the quality of the structure solution and subsequent refinement gives confidence that this is indeed the correct model. The structure was refined with reasonable atomic displacement parameters and close to 100% occupancy sum for the cationic sites. In addition, there was no evidence from reciprocal space reconstructions for doubling the unit cell, which could lead to a higher symmetry. After thorough analysis of the diffraction frames, several unindexed reflections were identified to be the result of twinning. The twinning matrix is listed in Table 4. For the peak-extraction procedure and subsequent integration of the data, the weaker twin domain was neglected. Twin matrix was later used in the refinement to resolve partially separated, fully separated, and fully overlapped reflections. Out of a total of 10626 reflections integrated for the larger twin domain, 3335

TABLE 4. Summary of data collection conditions and refinement parameters for pseudojohannite

Structural formula	Single crystal, White Canyon sample $Cu_3(OH)_2[(UO_2)_4O_4(SO_4)_2](H_2O)_{12}$
Unit-cell parameters (based on 5580 reflections)	
a, b, c (Å)	8.6744(4), 8.8692(4), 10.0090(5)
α, β, γ (°)	72.105(4), 70.544(4),76.035(4)
V (Å^3)	682.61(5)
Z	1
Space group	$P\bar{1}$
Temperature	293 K
Diffractometer	Oxford Gemini, Atlas CCD detector
Wavelength	Mo$K\alpha$, 0.7107 Å
Crystal dimensions	0.102 x 0.069 x 0.021 mm
Collection mode	ω scans to fill Ewald sphere
Limiting θ angles	2.86–29.38°
Limiting Miller indices	$-11 < h < 11$, $-12 < k < 12$, $-13 < l < 13$
No. of reflections	10,626
No. of unique reflections	3335
No. of observed reflections (criterion)	2264 [$I_{obs} > 3\sigma(I)$]
Absorption correction (mm^{-1}), method	26.50, analytical
R_{int} on F^2	0.0476
F_{000}	758
* Refinement by Jana2006 on F^2	
Parameters refined	169
R_{obs}, wR_{obs}	0.0347, 0.0704
R_{all}, wR_{all}	0.0481, 0.0771
GOF (obs)	1.28
Weighting scheme, details	σ, $w = 1/[\sigma^2(I) + 0.0004I^2]$
$\Delta\rho_{min}$, $\Delta\rho_{max}$ (e/Å^3)	4.71 (close to U1), –1.77
Twinning matrix	$\begin{pmatrix} -1 & 0 & 0 \\ 0 & -1 & 0 \\ -3/5 & -3/5 & 1 \end{pmatrix}$

reflections were unique, and 2664 of the unique reflections were classified as observed [with criterion $I_{obs} > 3\sigma(I)$]. The data were corrected for background, Lorentz and polarization effects, and an analytical absorption correction ($\mu = 26.16$ mm^{-1}) was applied, based on Clark and Reid (1995) implemented in the CrysAlis Pro package (Agilent Technologies 2010). The resulting R_{int} for the data was 0.0476. The crystallographic data and the details of the data collection are summarized in Table 4. (A CIF[1] is available.)

The crystal structure of pseudojohannite was solved by the charge-flipping method using the Superflip program (Palatinus and Chapuis 2007) and subsequently refined by the software JANA2006 (Petříček et al. 2006). The presence of the center of symmetry was suggested by the Gral algorithm of the CrysAlis Pro software, confirmed by the Superflip program and verified by the crystal-structure refinement. The structure solution provided positions of all atoms, except some adhering to O atoms belonging to H_2O. The majority of the atoms in the structure were refined using anisotropic atomic displacement parameters (ADP). Occupancies of the Cu sites were refined and their sums accounted practically for full occupancy of the sites (see Table 5). All non-hydrogen atoms were found; the maxima readable from the difference Fourier maps in the vicinity of the uranium atoms probably belong to the artifacts due to twinning. The refinement converged with the final $R_{obs} = 0.0347$, $R_{all} = 0.0481$, and a GOF = 1.28. The statistical indices and details for the refinement are listed in Table 3. The atomic positions and displacement parameters are listed in Table 5. For the crystal structure graphics the DIAMOND program (Crystal Impact; Brandenburg and Putz 2005) was used.

Crystal-structure description

The asymmetric unit of pseudojohannite contains 22 atoms, located on 2*i* sites of the triclinic space group $P\bar{1}$, except for the Cu1 atom, which sits on the 1*d* site. There are two distinct, symmetrically unique U atoms, two symmetrically unique Cu atoms, one S atom and 17 O atoms, 6 of the latter belonging to H_2O groups and one to an OH group. Each U atom is strongly bonded to two axial O atoms forming the $(UO_2)^{2+}$ uranyl ion with U-O_{Ur} bond lengths ranging between 1.81 and 1.83 Å. Each uranyl ion is additionally coordinated by five O atoms, designated as O_{eq}, located at the equatorial vertices of the pentagonal bipyramids. The U-O_{eq} bond-lengths for the UO_7 pentagonal bipyramids vary from 2.25 to 2.51 Å. These values are reasonably consistent with those given by Burns et al. (1997) and Burns (2005) for pentagonal uranyl bipyramidal coordination, 2.37(9) Å. The S atom is tetrahedrally coordinated, with bond lengths in the range of 1.47 to 1.48 Å, consistent with the S-O distances in sulfate groups (Hawthorne et al. 2006).

From the two symmetrically unique Cu sites, the one denoted Cu1 is coordinated by six ligands forming a strongly tetragonally distorted octahedron with C_{4v} symmetry, characterized by four shorter equatorial bonds and two longer axial bonds (Table 6), typical for the Jahn-Teller effect of Cu(II) (Jahn and Teller 1937; Burns and Hawthorne 1995; Hawthorne and Schindler 2000). The second site, Cu2, is coordinated by 5 ligands, comprising one long and four shorter bonds characteristic of the square pyramidal coordination, also typical for the Jahn-Teller effect of Cu(II) (Burns and Hawthorne 1995).

Bond-valence analysis, structural connectivity, and structural formula

Calculated bond-valence sums (according to Brown 2002) for the crystal structure of pseudojohannite (Table 7) confirm that the cations U and S are present in hexavalent forms, and that Cu clearly is present in divalent form, consistent with its Jahn-Teller distorted coordination.

Pseudojohannite possess a layered sheet structure with a uranyl sulfate structural sheet, Cu^{2+}-Φ polyhedra plus a single H_2O molecule in the interlayer (Fig. 3). The structural sheets

[1] Deposit item AM-12-072, CIF. Deposit items are available two ways: For a paper copy contact the Business Office of the Mineralogical Society of America (see inside front cover of recent issue) for price information. For an electronic copy visit the MSA web site at http://www.minsocam.org, go to the American Mineralogist Contents, find the table of contents for the specific volume/issue wanted, and then click on the deposit link there.

Table 5. Atomic coordinates and displacement parameters (in Å^2) for crystal structure of pseudojohannite (based on single-crystal data)

Atom	x	y	z	U_{eq}	U_{11}	U_{22}	U_{33}	U_{23}	U_{13}	U_{12}
U1	0.42802(4)	0.34306(4)	0.46462(4)	0.0077(1)	0.0064(2)	0.0066(2)	0.0105(2)	−0.0013(1)	−0.0028(1)	−0.0020(2)
U2	0.09013(4)	0.67616(4)	0.47194(4)	0.0083(1)	0.0062(2)	0.0064(2)	0.0125(2)	−0.0011(1)	−0.0030(1)	−0.0023(2)
Cu1*	0.5	0	0	0.0145(7)	0.018(1)	0.014(1)	0.012(1)	−0.0052(7)	−0.0063(7)	0.0011(8)
Cu2*	−0.0072(2)	0.1684(2)	−0.0069(1)	0.0167(5)	0.0143(7)	0.0165(7)	0.0161(8)	−0.0027(5)	0.0003(5)	−0.0044(6)
S	0.7502(3)	0.0037(3)	0.4954(3)	0.0103(9)	0.008(1)	0.009(1)	0.016(1)	−0.0019(9)	−0.004(1)	−0.005(1)
O1	0.5709(8)	0.0786(8)	0.1290(7)	0.017(3)	0.026(4)	0.017(4)	0.014(4)	−0.003(3)	−0.010(3)	−0.005(3)
O2	0.3516(8)	0.5917(8)	0.4981(7)	0.012(1)						
O3	−0.1183(8)	−0.0130(9)	0.1189(8)	0.018(3)	0.010(3)	0.025(4)	0.018(4)	−0.002(3)	−0.001(3)	−0.009(3)
O4	0.2056(9)	0.1178(9)	0.1158(8)	0.024(3)	0.023(4)	0.025(4)	0.022(4)	−0.003(3)	−0.007(3)	−0.005(4)
O5	0.1505(7)	0.4083(8)	0.5051(7)	0.010(1)						
O6	0.4796(8)	0.4253(8)	0.2692(7)	0.016(3)	0.021(4)	0.013(3)	0.011(4)	−0.006(3)	−0.004(3)	0.002(3)
O7	0.311(1)	0.420(1)	0.062(1)	0.040(4)	0.042(5)	0.034(5)	0.046(6)	0.000(4)	−0.022(4)	−0.007(5)
O8	0.3804(8)	0.2360(8)	0.6585(7)	0.014(3)	0.015(4)	0.014(3)	0.011(4)	−0.004(3)	−0.004(3)	−0.001(3)
O9	0.4754(8)	−0.2140(8)	0.1374(8)	0.019(3)	0.021(4)	0.016(4)	0.018(4)	−0.011(3)	−0.004(3)	0.002(3)
O10	−0.160(1)	0.321(1)	0.1013(9)	0.031(3)	0.033(5)	0.028(4)	0.024(5)	−0.004(4)	0.005(4)	−0.012(4)
O11	0.1621(8)	0.7036(8)	0.2755(7)	0.016(3)	0.017(4)	0.015(4)	0.016(4)	0.000(3)	−0.004(3)	−0.005(3)
O12	0.6657(8)	0.1326(8)	0.3982(7)	0.016(2)						
O13	0.1013(9)	0.3492(9)	−0.1471(8)	0.024(3)	0.023(4)	0.020(4)	0.025(5)	−0.005(3)	−0.001(3)	−0.004(4)
O14	0.0156(8)	0.6725(9)	0.6640(8)	0.019(3)	0.013(4)	0.025(4)	0.017(4)	0.000(3)	−0.002(3)	−0.005(3)
O15	0.7932(8)	0.0726(8)	0.5931(7)	0.015(2)						
O16	0.6428(8)	−0.1150(8)	0.5913(7)	0.013(1)						
O17	0.8984(8)	−0.0764(8)	0.4047(7)	0.014(2)						

* Refined occupancies for Cu1 and Cu2 are 0.983(7) and 0.977(5), respectively. U_{eq} is defined as a third of the trace of orthogonalized U_{ij} tensor. The anisotropic displacement factor exponent takes the form: $-2\pi^2[h^2 a^{*2}U_{11} + ... + 2hka^*b^*U_{12}]$.

TABLE 6. Selected interatomic distances and polyhedral geometries for the crystal structure of pseudojohannite (based on single-crystal data)

U1-O6	1.805(6)	U2-O11	1.809(7)
U1-O8	1.833(6)	U2-O14	1.805(7)
U1-O2	2.397(7)	U2-O2	2.286(7)
U1-O2	2.296(8)	U2-O5	2.249(6)
U1-O5	2.262(6)	U2-O5	2.302(7)
U1-O12	2.484(6)	U2-O15	2.485(8)
U1-O16	2.511(8)	U2-O17	2.472(6)
$<O_{Ur}$-U-$O_{Ur}>$	173.2(2)	$<O_{Ur}$-U-$O_{Ur}>$	173.7(2)
$<U-O_{Ur}>$	1.819	$<U-O_{Ur}>$	1.807
$<U-O_{eq}>$	2.390	$<U-O_{eq}>$	2.359
S1-O12	1.476(7)		
S1-O15	1.478(9)		
S1-O16	1.468(7)		
S1-O17	1.470(6)		
<S1-O>	1.473		
Δ	0.030		
σ^2	4.239		
ECoN	3.999		
Cu1-O1	1.955(9) ×2	Cu2-O3	1.949(7)
Cu1-O4	2.538(7) ×2	Cu2-O3	1.936(8)
Cu1-O9	1.984(6) ×2	Cu2-O4	2.426(9)
<Cu1-O>	2.159	Cu2-O10	1.959(8)
V_{Cu}	13.071 Å^3	Cu2-O13	1.973(7)
Δ	0.117	<Cu2-O>	2.040
σ^2	9.353	V_{Cu}	6.410 Å^3
ECoN	4.133	Δ	0.074
		ECoN	4.154

Notes: Δ = Bond-length distortion after Brown and Shannon (1973); σ^2 = bond-angle distortion after Robinson et al. (1971); ECoN = an effective coordination number after Hoppe (1979); V_{Cu} = polyhedral volume (in Å^3). Calculations by Vesta software (Momma and Izumi 2008).

TABLE 7. Bond-valence analysis for the crystal structure of pseudojohannite

	U1	U2	Cu1	Cu2	S	∑BV	Assign.
O1			0.47×2↓			0.47	H_2O
O2	0.68, 0.61	0.62				1.91	O
O3				0.48, 0.50		0.98	OH
O4			0.10×2↓	0.13		0.23	H_2O
O5	0.65	0.60, 0.67				1.92	O
O6	1.60					1.60	O
O7						0.00	H_2O
O8	1.52					1.52	O
O9			0.44×2↓			0.44	H_2O
O10				0.47		0.47	H_2O
O11		1.59				1.59	O
O12	0.42				1.49	1.91	O
O13				0.45		0.45	H_2O
O14		1.60				1.60	O
O15		0.42			1.48	1.90	O
O16	0.40				1.52	1.92	O
O17		0.43			1.52	1.95	O
∑BV	5.88	5.93	2.02	2.04	6.01		

Notes: Values are expressed in valence units (v.u.). ∑BV = bond-valence sums; ×2↓ = multiplicity. U^{6+}-O bond strengths ($r_0 = 2.045$, $b = 0.51$) from Burns et al. (1997); Cu^{2+}-O and S^{6+}-O bond strengths from Brown and Altermatt (1985).

are of zippeite topology, where uranyl pentagonal bipyramids form chains by sharing equatorial edges between two uranyl bipyramids. Adjacent chains are then linked via shared equatorial vertices of the uranyl bipyramids and sulfate tetrahedra to form these sheets (Fig. 4). Such sheets were found both in the synthetic (Vochten et al. 1995; Burns et al. 2003) and natural (Plášil et al. 2011a) zippeite, in synthetic zippeite-group phases (Burns et al. 2003), in synthetic zippeite phases with mixed univalent and divalent cations (Peeters et al. 2008), in marécottite (Brugger et al. 2003), and in sejkoraite-(Y) (Plášil et al. 2011b).

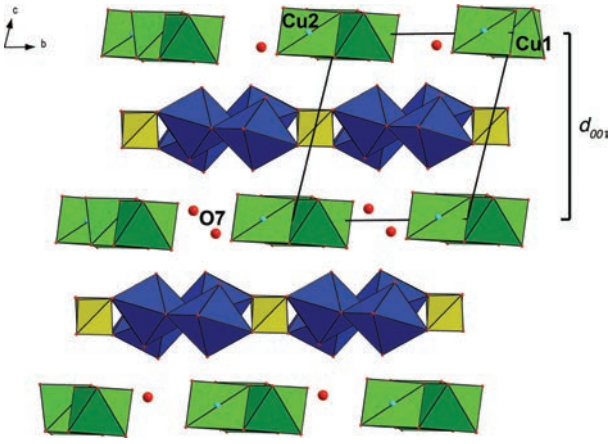

FIGURE 3. Crystal structure of pseudojohannite viewed along [100]. Structural sheets of zippeite topology consisting of uranyl pentagonal bipyramids (blue) and sulfate tetrahedra (yellow) alternate with interlayers, where a chains of copper (both green) octahedra (Cu1) and square bipyramids (Cu2) together with H_2O molecules (O7) bonded only via hydrogen bonds are located. Unit-cell edges outlined. (Color online.)

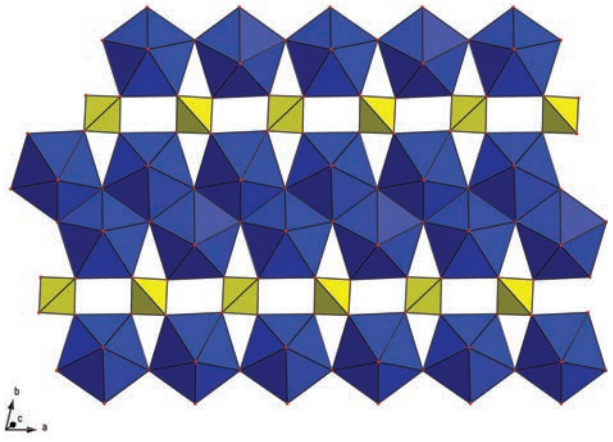

FIGURE 4. Uranyl-sulfate sheet of zippeite topology of the composition $[(UO_2)_4O_4(SO_4)_2]^{4-}$ found in the crystal structure of pseudojohannite. (Color online.)

Bond-valence analysis indicates that there is no OH within the structural sheet. Sheets of the zippeite uranyl anion topology in the structure of pseudojohannite are characterized by the composition $[(UO_2)_4O_4(SO_4)_2]^{4-}$.

In the interlayer space, $[Cu_3(OH)_2(H_2O)_{12}]^{4+}$ chains run parallel to [100], and comprise pairs of $Cu2\Phi_5$ square pyramids (Fig. 5) joined through edge-sharing where the edge is generated by two O3 atoms (which are related by a center of symmetry located at the center of this edge). These pairs are bridged at the pyramid apices through corner-sharing with the $Cu1\Phi_6$ octahedron (Fig. 5). Bond-valence analysis (Table 7) indicates that O3 belongs to OH group and an additional proton must be shared by several sites to reach a charge balance; the remaining Cu-ligands are H_2O groups. An additional water molecule fills the remaining volume within the interlayer space. A hydrogen-bonding net-

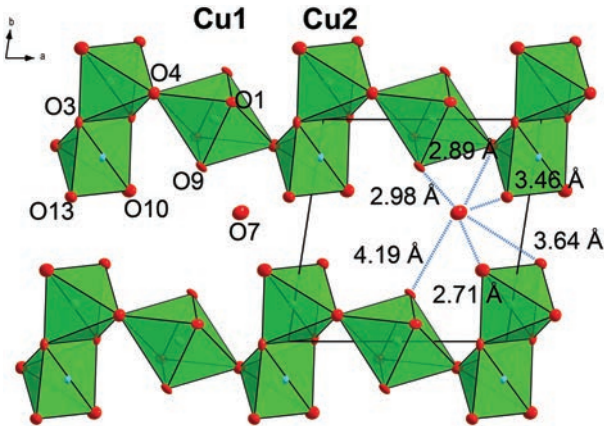

FIGURE 5. A chain of copper polyhedra in the structure of psedudojohannite, resulting from polymerization of bridging octahedra (Cu1) and dimers of square bipyramids sharing an edge (Cu2). Interatomic distances (in blue solid line) to O7 atom located between the layers are displayed. Atomic displacement parameters are drawn at the 50% probability level. (Color online.)

work (see further Discussion) provides the linkage between the structural sheets; these structural sheets are characterized by a considerable interplanar distance of 9.14 Å, mentioned also by Brugger et al. (2006). These weak interactions are responsible for the very good cleavage of pseudojohannite along (001), and thus correspond to the dominant diffraction peak in the powder pattern of pseudojohannite at ~9.15 Å (d_{001}, 100% of relative intensity in Bragg-Brentano geometry).

Based on results of the refinement and bond-valence analysis, the resulting structural formula of pseudojohannite is, $Cu_3(OH)_2[(UO_2)_4O_4(SO_4)_2](H_2O)_{12}$, $Z = 1$, assuming that the Cu sites are fully occupied (Table 4).

EXPERIMENTAL METHODS

High-resolution synchrotron powder diffraction on the holotype specimen

The green aggregates from the type specimen (P1P 1/2000) sample from Werner/Rovnost mine were mildly crushed under acetone and loaded into a 0.3 mm diameter glass capillary. Diffraction data were collected under ambient conditions on the powder diffraction beamline, 10-BM1 (Wallwork et al. 2007), at the Australian Synchrotron using the MYTHEN microstrip detector (Schmitt et al. 2003). The capillary was aligned concentric to the rotation axis of the 3-circle diffractometer. The wavelength used for the data collection was refined to ~0.7515 Å using NIST standard 660a, LaB_6. Data were collected over the 2θ range 3.0 to 83.5° using two detector positions. The resulting two data sets were combined using the in-house software "DataPro," and output on a grid of evenly spaced data points with the step size of 0.00375°. Attempts to solve crystal structure directly from the powder data prior to single-crystal experiment are described in Appendix 1.

Rietveld refinement

The Rietveld refinement based on the structure model obtained from the single crystal was fitted to the powder data using the TOPAS software v.4.2. Keeping atomic displacement parameters and Cu site occupancies as determined by the single-crystal study, the U and Cu2 atom positions were successfully refined. The following agreement factors were achieved: GOF 4.38, $R_{wp} = 0.0530$, $R_{exp} = 0.0121$; the refined heavy atom positions are listed in Table 8. Based on results of the Rietveld refinement and visual inspection of the measured and calculated powder profile we can consider the crystal structure of pseudojohannite from White Canyon to be identical to that from Jáchymov.

TABLE 8. Refined coordinates for U and Cu atoms obtained from the Rietveld refinement

Atom	x	y	z	B_{eq}
U1	0.4277(1)	0.3420(1)	0.4653(1)	0.608
U2	0.0901(1)	0.6766(1)	0.4724(1)	0.655
Cu1	0.5	0	0	1.145
Cu2	−0.0081(4)	0.1698(4)	−0.0066(4)	1.319

Notes: Refinement based on atomic coordinates from single-crystal XRD. Refined unit-cell parameters: $a = 8.68239(3)$, $b = 8.87811(3)$, $c = 10.02136(4)$ Å, $\alpha = 72.1257(3)°$, $\beta = 70.5266(3)°$, $\gamma = 76.0207(2)°$, and $V = 684.7395(45)$ Å^3. Indices of agreement GOF = 4.38, $R_{wp} = 0.0530$, $R_{exp} = 0.0121$.

DISCUSSION

The crystal structure of pseudojohannite can be represented by the structural unit $[(UO_2)_4O_4(SO_4)_2]^{4-}$ and the interstitial complex $[Cu_3(OH)_2(H_2O)_{12}]^{4+}$. The stability of the structure is maintained only via hydrogen-bonds between the structural sheet and interstitial complex. For the analysis of the bonding and bond-valence properties of those two units we used the procedure described in detail by Hawthorne and Schindler (2008), as well as Schindler and Hawthorne (2008).

The structural unit of pseudojohannite has an effective charge of 4, because no OH group is present within this sheet. As the structural unit contains 20 anions, the value of the charge-deficiency per anion (CDA) is 0.20 v.u., therefore, the corresponding Lewis basicity of the structural unit is within the range of 0.15–0.25 v.u. This range of values is characteristic for minerals and compounds of the zippeite topology (Schindler and Hawthorne 2008; Plášil et al. 2011a). A sheet of similar composition and the same bond-valence characteristics, $[(UO_2)_2(SO_4)O_2]^{2-}$, was previously found in magnesiozippeite, zinczippeite, and cobaltzippeite, $^{[6]}M^{2+}(H_2O)_3[(UO_2)_2(SO_4)O_2](H_2O)_{0.5}$ with M^{2+} = Mg, Zn, and Co (Burns et al. 2003).

The Lewis acidity of the interstitial complex $[Cu_3(OH)_2(H_2O)_{12}]^{4+}$ in pseudojohannite is 0.20 v.u., where the formal charge is 4, including an additional charge of 2, transferred by the hydrogen bonds. The total number of bonds within the interstitial complex is 30—counting Cu, OH, and H_2O. Here, we can see that the Lewis basicity of the structural unit is matching the Lewis acidity of the interstitial complex, thus fulfilling the demand of valence-matching principle for stability of the compound (Brown 1981, 2002, 2009).

In general, the interstitial complex may be described as $[^{[m]}M^{+}_{a}\ ^{[n]}M^{2+[l]}_{b}M^{3+}_{c}(H_2O)_d(H_2O)_e(H_2O)_{f^{[q]}}(OH)_g(H_2O)_r]^{(a+2b+3c-f)+}$, where M is any type of interstitial cation; d, e, and f denote the numbers of transformer, non-transformer, and inverse transformer (H_2O) groups; and r denotes the number of interstitial (H_2O) groups not bonded to interstitial cations (Schindler and Hawthorne 2008). From Figure 3 in Schindler and Hawthorne (2008) it is clear that for an interstitial complex having a Lewis acidity of 0.20 v.u. and containing [6]-coordinated M^{2+} cation, four transformers (H_2O) per cation are expected.

Analyzing the coordination of O atoms present in the OH and H_2O groups in the structure of pseudojohannite, we can see that the O atoms O1 and O9, coordinating Cu1 in the equatorial plane of the tetragonal bipyramid, should be [3]-coordinated. Therefore we can identify these O atoms ss transformer H_2O groups. The bridging O4 atom should then be [4]-coordinated, hence it is a non-transformer H_2O group. There are two OH groups within

the $Cu2\Phi_5$ polyhedra. Since they form a shared edge, they are [3]-coordinated. An additional two O atoms coordinated to Cu2 atoms, O10 and O13, are again [3]-coordinated, hence, they are also transformer H_2O groups. The remaining O atom, O7, in a non-coordinating H_2O group also represents a non-transformer group. In summary, the interstitial complex in pseudojohannite may be written as $^{[5]}Cu_2^{2+[6]}Cu^{2+[3]}(OH)_2(H_2{}^{[3]}O)_8(H_2{}^{[4]}O)_2(H_2O)_2$, which describes the coordination of the elements within the structure, as outlined above.

Hydrogen-bonding provides a linkage between the structural sheets and the interstitial complex of the structure of pseudojohannite, which itself is characterized by a large interplanar distance of 9.14 Å (Fig. 3). This interplanar spacing is the third largest within the zippeite-like compounds, comparable to those found in marécottite, 9.47 Å (Brugger et al. 2003), and sejkoraite-(Y), 9.28 Å (Plášil et al. 2011b). Using bond-valence analysis (Table 7), it is possible to see that the undersaturated O atoms that may act as acceptors for hydrogen-bonds are the O_{Ur} atoms; these are characterized by a bond-valence deficiency of ~0.40 v.u. This value is consistent with an oxygen atom that is able to accept two H-bonds, of the bond length ~2.8 Å, each of 0.20 v.u. (Ferraris and Ivaldi 1988). A close inspection of the structure reveals that the O_{Ur} atoms, O6, O8, O14, and O11 have contacts to a range of OH or OH_2 O atoms, such that the Φ-H···O_{Ur} contact lengths are in the range 2.8–3.1 Å. Although it is not possible to ascertain the exact hydrogen bonding network from the current data set, the following possible bonding pathways can be identified: O6···O7/O9/O10, O8···O1/O3/O9/O13, O11···O9/O13, and O14···O4/O10/O13.

ACKNOWLEDGMENTS

We thank our friend and colleague Petr Ondruš for supporting this research. Joe Marty and Jaroslav Hyršl are highly acknowledged for providing access to the specimens used in this study. The comments of the anonymous reviewers, as well as the editorial handling by Hazhoe Liu are highly appreciated. This research was funded by the Grant of Ministry of Culture of the Czech Republic (DKRVO National Museum, Prague) to J.S. The project P204/11/0809 of the Czech Science Foundation to K.F., M.D., and J.P., the project P204/11/0809 of the Grant Agency of the Czech Republic and the EU-project "Research group for radioactive waste repository and nuclear safety" (CZ.1.07/2.3.00/20.0052) to R.Š. and J.P., also are highly acknowledged. This work was, in part, performed at the powder diffraction beamline at the Australian Synchrotron.

REFERENCES CITED

Altomare, A., Camalli, M., Cuocci, C., Giacovazzo, C., Moliterni, A., and Rizzi, R. (2009) EXPO2009: Structure solution by powder data in direct and reciprocal space. Journal of Applied Crystallography, 42, 1197–1202.

Brandenburg, K. and Putz, H. (2005) DIAMOND Version 3. Crystal Impact GbR, Postfach 1251, D-53002 Bonn, Germany.

Brown, I.D. (1981) The bond-valence method: an empirical approach to chemical structure and bonding. In M. O'Keeffe and A. Navrotsky, Eds., Structure and Bonding in Crystals II, p. 1–30. Academic Press, New York.

——— (2002) The Chemical Bond in Inorganic Chemistry: The Bond Valence Model, p. 230, 278. Oxford University Press, U.K.

——— (2009) Recent developments in the methods of the bond valence model. Chemical Reviews, 109, 6858–6919.

Brown, I.D. and Altermatt, D. (1985) Bond-valence parameters obtained from a systematic analysis of the inorganic crystal structure database. Acta Crystallographica, B41, 244–248.

Brown, I.D. and Shannon, R.D. (1973) Empirical bond-strength bond length curves for oxides. Acta Crystallographica, A29, 266–282.

Brugger, J., Burns, P.C., and Meisser, N. (2003) Contribution to the mineralogy of acid drainage of uranium minerals: Marécottite and the zippeite group. American Mineralogist, 88, 676–685.

Brugger, J., Wallwork, K.S., Meisser, N., Pring, A., Ondruš, P., and Čejka, J. (2006) Pseudojohannite from Jáchymov, Musonoï, and La Creusaz: A new member of the zippeite-group. American Mineralogist, 91, 929–936.

Bruker AXS (2008) TOPAS V4: General profile and structure analysis software for powder diffraction data. User's Manual, Bruker AXS, Karlsruhe, Germany.

Burns, P.C. (2005) U^{6+} minerals and inorganic compounds: Insights into an expanded structural hierarchy of crystal structures. Canadian Mineralogist, 43, 1839–1894.

Burns, P.C. and Hawthorne, F.C. (1995) Coordination geometry structural pathways in Cu^{2+} oxysalt minerals. Canadian Mineralogist, 33, 889–905.

Burns, P.C., Ewing, R.C., and Hawthorne, F.C. (1997) The crystal chemistry of hexavalent uranium: Polyhedron geometries, bond-valence parameters, and polymerization of polyhedra. Canadian Mineralogist, 35, 1551–1570.

Burns, P.C., Deely, K.M., and Hayden, L.A. (2003) The crystal chemistry of the zippeite group. Canadian Mineralogist, 41, 687–706.

Čejka, J. (1999) Infrared spectroscopy and thermal analysis of the uranyl minerals. In P.C. Burns and R. Finch, Eds., Uranium: Mineralogy, geochemistry and the environment, 38, 521–622. Reviews in Mineralogy, Mineralogical Society of America, Chantilly, Virginia.

Čejka, J., Urbanec, Z., Čejka, J. Jr., and Mrázek, Z. (1988) Contribution to the thermal analysis and crystal chemistry of johannite $Cu[(UO_2)_2(SO_4)_2(OH)_2].8H_2O$, Neues Jahrbuch fuer Mineralogie, Abhandlungen, 159, 297–309.

Clark, R.C. and Reid, J.S. (1995) The analytical calculation of absorption in multifaceted crystals. Acta Crystallographica, A51, 887–897.

Ferraris, G. and Ivaldi, G. (1988) Bond valence vs bond length in O…O hydrogen bonds. Acta Crystallographica, B44, 341–344.

Hawthorne, F.C. and Schindler, M. (2000) Topological enumeration of decorated $[Cu^{2+}\Phi_2]_N$ sheets in hydroxyl-hydrated copper-oxysalt minerals. Canadian Mineralogist, 38, 751–761.

——— (2008) Understanding the weakly bonded constituents in oxysalt minerals. Zeitschroft für Kristallographie, 223, 41–68.

Hawthorne, F.C., Huminicki, D.M.C., and Schindler, M. (2006) Sulfate minerals. I. Bond topology and chemical composition. Canadian Mineralogist, 44, 1403–1429.

Hoppe, R. (1979) Effective coordination number (ECoN) and mean-fictive ionic radii (Mefir). Zeitschrift für Kristallographie, 150, 23–52.

Jahn, H.A. and Teller, E. (1937) Stability of polyatomic molecules in degenerate electronic states. I. Orbital degeneracy. Proceedings of Royal Society, Seris A, 161, 220–235.

Mereiter, K. (1982) Die Kristallstruktur des Johannites, $Cu(UO_2)_2(OH)_2(SO_4)_2{\cdot}8H_2O$. Tschermaks Mineralogische und Petrographische Mitteilungen, 30, 47–57.

Momma, K. and Izumi, F. (2008) VESTA: A three-dimensional visualization system for electronic and structural analysis. Journal of Applied Crystallography, 41, 653–658.

Ondruš, P., Veselovský, F., Skála, R., Císařová, I., Hloušek, J., Frýda, J., Vavřín, I., Čejka, J., and Gabašová, A. (1997) New naturally occurring phases of secondary origin from Jáchymov (Joachimsthal). Journal of the Czech Geological Society, 42, 77–107.

Ondruš, P., Veselovský, F., Gabašová, A., Hloušek, J., and Šrein, V. (2003) Supplement to secondary and rock-forming minerals of the Jáchymov ore district. Journal of the Czech Geological Society, 48, 3-4, 149–155.

Palatinus, L. and Chapuis, G. (2007) Superflip – A computer program for the solution of crystal structures by charge flipping in arbitrary dimensions. Journal of Applied Crystallography, 40, 451–456.

Peeters, M.O., Vochten, R., and Blaton, N. (2008) The crystal structures of synthetic potassium-transition metal zippeite-group phases. Canadian Mineralogist, 46, 173–182.

Petříček, V., Dušek, M., and Palatinus, L. (2006) Jana2006. The crystallographic computing system. Institute of Physics, Praha, Czech Republic. http://jana.fzu.cz.

Plášil, J., Mills, S.J., Fejfarová, K., Dušek, M., Novák, M., Škoda, R., Čejka, J., and Sejkora, J. (2011a) The crystal structure of natural zippeite, $K_{1.85}H_{0.15}^{\circ}[(UO_2)_4O_2(SO_4)_2](H_2O)_4$, from Jáchymov, Czech Republic. Canadian Mineralogist, 49, 1089–1103.

Plášil, J., Dušek, M., Novák, M., Čejka, J., Císařová, I., and Škoda, R. (2011b) Sejkoraite-(Y), a new member of the zippeite group containing trivalent cations from Jáchymov (St. Joachimsthal), Czech Republic: Description and crystal structure refinement. American Mineralogist, 96, 983–991.

Pouchou, J.L. and Pichoir, F. (1985) "PAP" (φρZ) procedure for improved quantitative microanalysis. In J.T. Armstrong, Ed., Microbeam Analysis, 104–106. San Francisco Press, California.

Robinson, K., Gibbs, G.V., and Ribbe, P.H. (1971) Quadratic elongation: A quantitative measure of distortion in coordination polyhedra. Science, 172, 567–570.

Schindler, M. and Hawthorne, F.C. (2008) The stereochemistry and chemical composition of interstitial complexes in uranyl-oxysalt minerals. Canadian Mineralogist, 46, 467–501.

Schmitt, B., Bronnimann, C., Eikenberrya, E.F., Gozzo, F., Hormann, C., Horisberger, C., and Patterson, B. (2003) Mythen detector system. Nuclear Instruments and Methods in Physics Research, Section A, 501, 267–272.

Sokol, F. and Čejka, J. (1992) A thermal and mass spectrometric study of synthetic johannite. Thermochimica Acta, 206, 235–242.

Vochten, R., Van Haverbeke, L., Van Springel, K., Blaton, N., and Peetres, O.M.

(1995) The structural and physicochemical characteristics of synthetic zippeite. Canadian Mineralogist, 33, 1091–1101.
Wallwork, K.S., Kennedy, B.J., and Wang, D. (2007) The high resolution powder diffraction beamline for the Australian Synchrotron, AIP Conference Proceedings, 879, 879–882.

Manuscript received February 8, 2012
Manuscript accepted June 11, 2012
Manuscript handled by Haozhe Liu

Appendix 1

Initial attempts to determine the crystal structure of pseudojohannite from powder diffraction data were made using the larger triclinic cell (twice in volume to that determined from single-crystal diffraction) and were successful in ascertaining a reasonable structural model. The model for pseudojohannite structure was obtained, using a cell of the volume ~1380 Å^3 and the space group $P\bar{1}$, by combining direct methods with some additional modeling employing EXPO2009 (Altomare et al. 2009). Most default settings were used to extract I_{obs} from the data over the angle range $3.5° < 2\theta < 40.15°$ (number of reflections 1082); the single peak range was adjusted about the (200) reflection between 10.51–10.81° to allow for better definition of the peak shape. The pseudotranslational symmetry was not applied. The solution thus obtained located all of the elements heavier than oxygen, only requiring relabeling of "S1" to Cu and "Cu1" to S. Several O atoms were also located in reasonable positions, particularly those in the UO_5 equatorial plane and some corner-shared O atoms in the $Cu\Phi_n$ chains. The additional O atoms required were inserted or repositioned via modeling, however it was not possible to ascertain whether Cu2 should be [5]- or [6]-coordinated; a [6]-coordinated distorted octahedron was modeled. A further 2 O atoms, which link the $Cu\Phi_n$ chains were located using PLATON (Spek 2009). Due to the difficulties associated with refining light elements in the presence of heavy elements, only U and Cu atoms were then refined using TOPAS v4.2 (Bruker ASX 2008). There were two small excluded regions where minor impurity peaks have been ignored (i.e., at 2θ 4.98–5.05° and 12.87–12.92°). The angular range of the data used for refinement was 3.4–52.6° and the background was fit using a combination of 3 peaks phases and a third-order Chebychev polynomial. Constrained refinement converged to final indices of agreement GOF 5.16, $R_{wp} = 0.0625$, $R_{exp} = 0.0121$.

Overall, even if the solution from the powder diffraction data did not bring a true structure model (lacking complete information for O atoms), it provided a model good enough for general considerations about its crystal structure. Thus we are convinced that this example demonstrates how efficient the structure determination from a negligible amount of the sample (<1 mg) can be when using the high-resolution powder diffraction.